Articles

Specific anti-gastric cancer effects of a recombinant plasmid expressing nonstructural protein 1 of parvovirus H1

Di Zhao, MS, *Chenwen Cai,* BS, *Yuanyuan Wang,* MS, *Shudong Xiao,* MD, PhD, *Qing Zheng,* MD, PhD.

ABSTRACT

الأهداف: للتحقيق من استجابة هذا الورم إلى البارفو المستقل H-1البارفو (PV)مع القدرة على التكرار التحليلي التفضيلي في الخلايا السرطانية.

الطريقة: أجريت الدراسة في معهد شنغهاي للأمراض الجهاز الهضمي،الهند من عام 2009م —2012م. ويُعبر NS1 عن البلازميد والتي تدخل في خطوط خلايا المعدة أو الفئران التي تحمل معها طعوم الورم. تم قياس كابت نمو الورم من خلال تتبع العلامة الفلورية والاستنساخ المحددة. وتم قياس نمو الورم والتحقق أيضاً من دور خلية ديشوميوستاسيسdyshomeostasis من خلال قياس التدفق الخلوي. وتم قياس مستوى دورة الخلية المنتظمة على مستوى الاستنساخ والبروتين.

النتائج: قمعت خلايا سرطان المعدة بشكل فعال في المختبر أو في نماذج الفئران إكسينوجرافت (الطعم الأجنبي). وكان يعتمد كابت الورم NS1 ويحركها بلازميد NS1 في بعض الأنسجة الطبيعية،وخاصة في الرئتين،لم يكن مصحوباً بآثار جانبية ضارة. تم العثور على NS1 للقضاء على خلايا سرطان المعدة في مرحلة G0/G1 مع منظم دورة P21 المتراكم معه.

الخاتمة: يُمكن NS1 من منع نمو الخلايا التي تصيب سرطان المعدة في المختبر ونموذج إكسينوجرافت ربما من خلال تحريض منظم دورة الخلية P21. هذه النتائج تدعم تطوير المزيد من البروتين NS1بارفوفيرال باعتباره المستجيب لمكافحة السرطان.

Objectives: To investigate the responsiveness of gastric tumor cells to the nonstructural protein (NS)1 of parvovirus H1, which has a preferential lytic growth cycle in cancer cells.

Methods: This study was carried out in Shanghai Institute of Digestive Disease, Renji Hospital, Shanghai, China from 2009 to 2012. An NS1-expressing plasmid was introduced into gastric cell lines or nude mice bearing tumor grafts. Expression was monitored by tracking fluorescence tag and specific transcription. Tumor growth suppression was measured, and cell cycle dyshomeostasis was verified by flow cytometry. Cell cycle regulators' level was measured on both the transcription and protein level.

Results: Gastric cancer cells were efficiently suppressed in vitro, or in the xenograft mice model. The NS1 dependent tumor suppression was specific since plasmid-driven NS1 expression in some normal tissues, in particular, the lungs was not accompanied by adverse side effects. The NS1 expression was found to stall gastric cancer cells in the G0/G1 stage with accumulation of cycle regulator p21.

Conclusion: The NS1 expression can suppress gastric cancer cell growth both in vitro and in xenograft model, probably through induction of the cell cycle regulator p21. These results support further development of the parvoviral NS1 protein as an anti-cancer effector.

Despite improvement in diagnosis and treatment, gastric cancer is still one of the most common types of malignancy worldwide.[1] With 0.74 million fatalities per year, it remains the third leading cause of cancer related deaths in China,[1,2] which warrants extensive research for new therapeutic approaches. In this regard, oncolytic viruses, as reviewed by Patel and Kratzke,[3] appears to be promising, given their ability to infect, propagate in, and kill tumor cells while sparing non-transformed cells. Among members of the oncolytic virus family, rodent parvoviruses are of particular interest because of their natural oncotropism and safety.[4] Interestingly, the cytotoxic effects of parvoviruses can be recapitulated in vitro through the expression of a single viral component, the nonstructural protein (NS)1.[4] The NS1 is a multifunctional protein involved in viral DNA amplification and transcription, virion assembly and cytotoxicity.[5] The NS1 functioning relies on post-translational modifications of specific domains,[6] subcellular distribution,[7] and interaction with various host cell factors.[8] In this study, we used 2 commonly studied gastric cancer cell lines; SGC 7901 and MGC 80-3 to observe the anti-gastric cancer effects of a recombinant plasmid expressing nonstructural protein 1 of parvovirus H-1 (PV). Previous studies showed that NS1 was able to block the cell cycle at various stages (in particular, the G2/M phase),[9] cause specific cytoskeleton alterations,[10-12] stimulate intracellular reactive oxygen species (ROS) accumulation,[13] and activate distinct cell death pathways.[14] Recent evidence suggests that PV-induced tumor cell lysis can also result in the activation of immune cells (including natural killer and dendritic cells), presumably through the release of tumor associated antigens, and viral or cellular immuno-stimulating molecular ligands.[15,16] Our previous work suggests that both infection with PV and transfection with NS1 could inhibit gastric cancer cells in vitro, and this suppression seemed to be related to the proliferation status of the cell lines. However, the exact mechanisms, as well as their effects in vivo remains unknown.[17] The goal of the present follow-up study was 2-fold. On a fundamental level, we investigated the mechanism responsible for the cytostatic effect of NS1 on human gastric tumor cells. On a more applied level, this work aimed to validate the use and safety of an expression plasmid for the delivery of NS1, and the suppression of heterotopic gastric tumors in the absence of adverse side effects, despite the plasmid-driven forced expression of NS1 in some normal tissues.

Methods. This study was carried out mainly in Shanghai Institute of Digestive Disease, Shanghai, China from September 2009 to December 2012. The animals were raised in the animal center of Tongji University, Shanghai, China. Prior related research information was retrieved by searching PubMed, EMBASE, Cochrane database, ClinicalTrials.gov, Google Scholar, and the International Continence Society (ICS) website using keywords "Nonstructural protein 1", "Oncolysis" and "Parvovirus".

Cell culture. The cell lines SGC 7901 and MGC 80-3 established from human gastric adenocarcinoma were obtained from Shanghai Institute of Cell Biology of Chinese Academy of Sciences (Shanghai, China). Cells were kept in humidified incubator with 5% CO_2 in PRMI1640 (GIBCO, Grand Island, NY, USA) medium supplemented with 10% (v/v) fetal bovine serum (GIBCO, Grand Island, NY, USA). Cells were trypsinized when reaching 90% confluency. All culture wares were purchased from Corning Inc (One Riverfront Plaza, Corning, NY, USA).

Plasmid construction and liposome-mediated transfection. The pEGFP-C1-NS1 was generated through amplification of the NS1 gene from parvovirus H-1 DNA, which was kindly provided by the German Cancer Research Center (Heidelberg, Germany), and cloning into pEGFP-C1 vector (CLONTECH, Palo Alto, CA, USA) using XhoI and BamHI restriction sites under control of cytomegalovirus (CMV) promoter. The primers used were: 5'-TCCGCTCGAGCTATGGC TGGAAACGCTTACTC-3,' and 5' - A T C G G G A T C C T T A G T C C A A G G T CAGCTCCTCGT-3'. The pcDNA3.1-NS1 was generated as previously described by Wang.[17] The real time-polymerase chain reaction (RT-PCR) products were separated by 1% agarose (Beyotime, Shanghai, China) gel electrophoresis. The recombinant plasmid was confirmed by DNA sequencing. Lipofectamine2000 (Invitrogen, Carlsbad, CA) mediated transfection procedure was performed as recommended by the manufacturer. A 1×10^5 cells/well were grown overnight in a 6-well plate. For each well, 4 ug DNA and 10 ul of liposome suspension were added to Opti-MEM (Invitrogen, Carlsbad, CA, USA) medium in a final volume of 500 ul. The transfection complex was incubated for at least 4 hours before replacement with complete culture medium. Expression of NS1 was confirmed by RT-PCR and fluorescence microscopy. Cells transfected with pEGFP-C1 were used as a mock control group. Blank controls were treated with the same volume of phosphate buffered saline (PBS) (GIBCO, Grand Island, NY, USA).

Growth curve measurement. Transfected cells were trypsinized into single cells and seeded in 16 25 cm^2 culture flasks at a concentration of 10^4 cells/ml. Four flasks were trypsinized and quantified every 24 hours for 4 days post transfection. A 300 ug/ml G418 (Beyotime, Shanghai, China) was supplemented to the medium from the second day on to eliminate non-transfected cells. Cell viability was determined by trypan blue (Sigma, St Louis, MO, USA) staining. The assay was performed in duplicate.

Detection of intracellular accumulation of ROS. Intracellular ROS level was detected using Dichlorofluorescein diacetate (DCFH-DA) (Beyotime, Shanghai, China), which was converted into a green fluorescent molecule in the presence of ROS. Cells transfected with NS1-expressing pcDNA3.1-NS1, or empty carrier pcDNA3.1 were seeded in a 6-well plate, and analyzed before reaching 80% confluency. Cells were washed thoroughly with PBS, and 2 ml 10 uM DCFH-DA were added to each well. After incubation at 37°C for 20 minutes, cultures were washed extensively with PBS to remove free DCFH-DA. Cells were then examined under inverted fluorescence microscope to assess ROS levels.

Cell cycle analysis. At least 5x10^5 transfected cells were trypsinized and fixed at a 24-hour intervals with 70% ice-cold ethanol. Cells were then stained with 50 ug/ml propidium iodide (PI) (Sigma, St Louis, MO, USA) for 30 minutes, and subjected to flow cytometry using an LSRFortessa analyzer (BD Biosciences, Franklin Lakes, NJ, USA). Fluorescence signals of both enhanced green fluorescent protein (EGFP), and PI were recorded using Flowcytometry Diva software (BD Biosciences, Franklin Lakes, NJ, USA). At least 10,000 counts were made for each sample. The cell cycle phase distribution was analyzed using the ModFit software (Verity Software House, Inc., Topsham, ME, USA). For the experimental groups, only cells positive for EGFP were taken into consideration.

Nude mice model. Four-week-old specific pathogen free (SPF) grade male nude mice were obtained from Shanghai Slac Laboratory Animal Co. Ltd. (Shanghai, China). Animals were kept in an environmentally controlled breeding room (temperature: 20±2°C; humidity: 60±5%; 12 hour dark/light cycle). The study was carried out in strict accordance with the recommendations of the animal center of Tongji University. The SGC7901 cells were trypsinized into single cells, and re-suspended in PBS. A total of 2x10^7 SGC7901 cells in 300 ul were subcutaneously injected into the axillary fossa of nude mice. Fourteen days after injection, mice with xenograft reaching approximately 0.5x0.5 cm were randomized into NS1, mock control, and blank control groups (n=5).

Jet-PEI mediated in vivo transfection. In vivo transfection using in vivo jet-PEI (PolyPlus-Transfection, Illkirch, France) was carried out according to the manufacturer's instruction. A total of 10 ug plasmid (recombinant plasmid for the experimental group, and vector only for the mock control group), and 1.2 ul reagent was added to a 5% (v/v) glucose solution in a final volume of 50 ul. The complex was kept on ice for almost 6 hours before being injected intra-tumorally into the mice. Mice from the blank control group received the same volume of saline. Injection was performed 6 times in a 72-hour interval. All the mice were sacrificed on the second day after the last injection by cervical dislocation. Tumor samples were dissected, and dimensions were measured.

Detection of NS1 expression in vivo. Twenty-four hours after in vivo transfection, mice were anesthetized via intra-peritoneal injection of 3.5% chloral hydrate at a dose of 10 ul/g. The EGFP-NS1 fusion protein were visualized at an excitation wavelength of 490 nm using a NightOWL II LB 983 NC100 imaging system (Berthold Technologies, Bad Wildbad, Germany). After the sacrifice, tumors were removed, fixed in 10% formaldehyde, and processed for histological examination of NS1 expression. Samples allocated to total ribonucleic acid (RNA) extraction were stored in liquid nitrogen.

Total RNA extraction, reverse transcription and RT-PCR. Total RNA was extracted from cultured cells or xenografts using TRIzol (Invitrogen, Carlsbad, CA) according to the manufacturer's protocol. A one ug total RNA was reversely transcribed into cDNA using PrimeScript RT reagent Kit (Takara, Biotechnology, Otsu, Shiga, Japan). The reverse transcription conditions were 37°C for 15 minutes, and 85°C for 5 seconds. Products were stored at -20°C before quantification. The RT-PCR using SYBR Premix Ex Taq (Takara Biotechnology, Otsu, Shiga, Japan) was carried out as follows: 95°C for 30 seconds; then 40 cycles at 95°C for 5 seconds and 60°C for 30 seconds. The products were confirmed by electrophoresis on 2% agarose gel, and visualized by ethidium bromide dye (Beyotime, Shanghai, China) staining. The following list summarizes the primer pairs used for RT-PCR analysis: for NS1, 5'-TCCACCAAGGGACGG AGGCTATTT -3' (forward) and 5'-ATTCTGCCGCGC TTAGCTTCCT-3' (reverse); for P21, 5' -ACAGCAGAGGAAGA CCATGTGGA -3' (forward), and for glyceraldehyde-3-phosphate dehydrogenase (GAPDH), 5' -AACCATGAGAAG TATGACAACA

-3' (forward) and 5'-CATGTGGGCCATGAGG TCCACC -3' (reverse). The GAPDH served as an internal control.

Protein immuno-detection. Cultured cells transfected with NS-1 expressing or empty vectors were lysed with radioimmunoprecipitation assay buffer (RIPA buffer) (Beyotime, Shanghai, China). After centrifugation supernatants were collected. Protein concentrations were measured using bi-cinchoninic acid (BCA) assay (Beyotime, Shanghai, China) according to the manufacturer's instruction. A total of 30 ug of protein extracts were fractionated by discontinuous sodium dodecyl sulfate polyacrylamide gel electrophoresis (SDS-PAGE), and blotted onto polyvinylidene difluoride (PVDF) membranes (Millipore, Bedford, MA, USA). After being blocked, membranes were incubated overnight at 4°C with primary antibodies specific for the following proteins: NS1 (1:4000), p21 (1:3000; EPITOMICS, Burlingame, CA, USA), cyclin-dependent kinases (cdk)2 (1:2300, EPITOMICS, Burlingame, CA, USA), E1 (1:1000, EPITOMICS, Burlingame, CA, USA), RB (1:1000, EPITOMICS, Burlingame, CA, USA), GAPDH (1:1000, EPITOMICS, Burlingame, CA, USA). Membranes were then stained with peroxidase-conjugated goat anti-rabbit antibodies (1:5,000; KangChen, Shanghai, China) for one hour at room temperature. The membranes were then washed, and visualized with the ECL detection kit (Pierce, Rockford, IL, USA).

Immunohistochemistry. Dissected samples were fixed overnight in 10% paraformaldehyde, and cut into 5-10 mm thick slides. After a microwave repair and intensive wash with PBS, samples were blocked with normal goat serum (Maxim, Fuzhou, China) to reduce unspecific binding. Slides were incubated at 4°C with primary rabbit antibodies specific for NS1 (1:1800). On the second day, slides were washed extensively with PBS supplemented with 0.1% tween-20, and incubated for one hour with HRP conjugated goat anti-rabbit secondary antibodies (Maxim, Fuzhou, China) diluted 1:200 in PBS. Cells positive for NS1 were visualized using the HRP-DAB kit (Maxim, Fuzhou, China). Cell nuclei were stained with hematoxylin for 30 seconds at room temperature. After the cover slides mounting, samples were analyzed using an Olympus BX51 microscope.

Statistics. The Statistical Package for Social Sciences version 13 software (SPSS Inc, Chicago, IL, USA) was used to compare means. Differences between groups were evaluated using the independent-samples t test. A $p<0.05$ was considered statistically significant.

Results. The NS1 expression inhibits the growth of human gastric cancer cell lines in culture. From a previous study, it was concluded that the NS1 protein needs to be phosphorylated at specific sites near its C-terminal in order to exert cytotoxic effect.[11] Therefore, the EGFP tag was added to the N-end of the NS1 protein. In vitro transfection was mediated by lipofectamin 2000, and evaluation of NS1 gene expression was performed by examining fluorescent cells under the microscope. As show in **Figure 1A**, the transfection efficiency was approximately 80% in both treated cell lines. Green fluorescence could be seen as early as 4 hours after transfection, and reached its peak approximately 24-36 hours post transfection. Compared to the mock control group, which only received EGFP-tagged empty carrier, EGFP-fused NS1 showed clear accumulation within the cell nuclei for approximately 72 hours until the signal faded away. This was in agreement with the preferential intra-nuclear localization of NS1. From 16-24 hours after transfection, both SGC 7901 and MGC 80-3 cells from the NS1 group underwent significant death as evidenced by cell lysis (**Figure 1B**). In contrast to the control (pEGFP-C1-treated) culture, pEGFP-C1-NS1 transfected cells from the moderately differentiated SGC 7901 line showed a marked decrease of growth rate ranging from 45-77% at day one-, and day 4-post transfection (**Figures 1C & 1D**). In the poorly differentiated line MGC 80-3, growth inhibition rates at day one was 73%, and 95% at day 4 after the pEGFP-C1-NS1 transfection. Cells transfected with empty pEGFP-C1 carrier had a growth curve similar to that of the parented cells.

The NS1 induces cell growth inhibition via G0/G1 phase arrest. We first investigated whether gastric cancer cell death was associated with intracellular accumulation of ROS, as previously demonstrated in HEK-293 and HeLa cells.[16] A clear ROS induction could be detected in the NS1 group, yet only from 28 hours post transfection. As mentioned above, gastric cancer cell death appeared prior to this time point (as early as 16-24 hours post transfection), suggesting that in these cells intracellular ROS production did not mediate NS1 cytotoxicity, and may rather be a late consequence of the cell death process.

This contrasts with the sequence of events observed in NS1-expressing HeLa cells, exemplifying the cell dependence of NS1 cytotoxic activities. We concluded that in gastric cancer cells, NS1 may act through a process different from the DNA damage check point pathway resulting in G2 arrest of the cell cycle. These results prompted us to investigate the interference of the NS1 protein with gastric cancer cell cycle. Cells
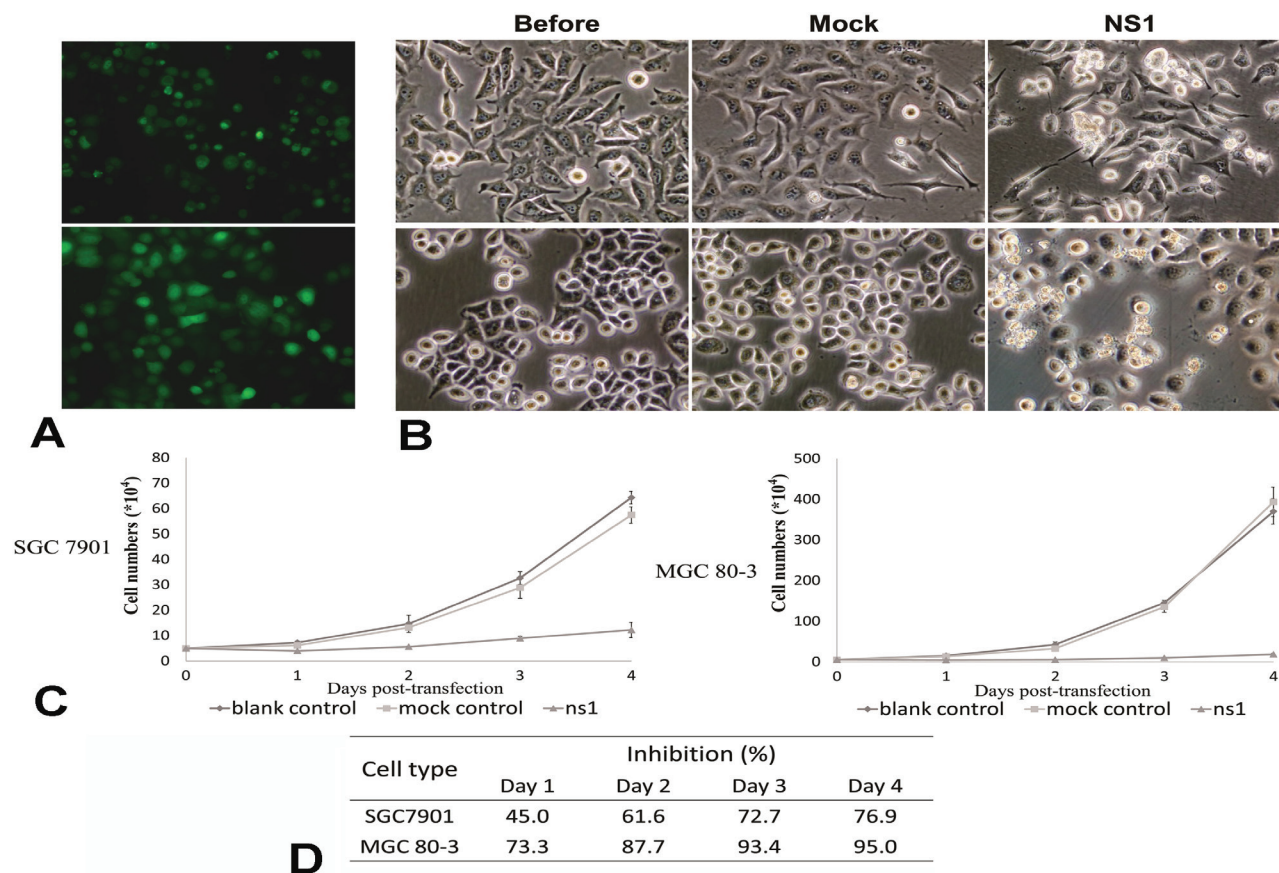
Figure 1 - In vitro inhibition of gastric cancer cell lines followed by forced expression of nonstructural protein (NS)1: **A)** fluorescence microscopy analysis of SGC 7901 cells 24 hours after transfection with p enhanced green fluorescent protein (EGFP)-C1-NS1 (upper panel) or pEGFP-C1 (lower panel) (200x); **B)** microscopic appearance of gastric cancer cells before, and 24 hours after transfection with pEGFP-C1 (mock) or pEGFP-C1-NS1 plasmids, upper panel: MGC 80-3 cells, lower panel: SGC7901 cells (200x); **C)** growth inhibition of gastric cancer cells expressing NS1, left: growth curve of SGC 7901 cultures, right: growth curve of MGC 80-3 cultures; and **D)** inhibition percentages calculated from the relative numbers of living cells in pEGFP-C1-NS1 versus pEGFP-C1 treated cultures.

were starved for at least 16 hours before transfection to achieve synchronization. To determine whether NS1 caused sustained cell cycle perturbations, cells were harvested at 24, 48, and 72 hours after transfection. To restrict the analysis to successfully transfected cells, samples were gated on the EGFP-expressing population. As shown in **Figure 2**, from 24 hours post transfection, NS1-expressing gastric cancer cells were strongly trapped in the G0/G1 phase, which was accompanied by a significant decrease in both S and G2/M subpopulations. Cell cycle arrest persisted over the 72 hours observation period, and represented, therefore, a long-lasting cell response to NS1 expression. In contrast, cells transfected with empty carrier and EGFP-negative cells in the NS1 group had the same cell cycle distribution as untreated cells. We can conclude that the cytostatic effect of NS1 was specific,

and not due to interference of the pEGFP-C1 carrier, or transfection procedure. Similar results were obtained with both gastric cancer cell lines.

The NS1 expression suppresses growth of heterotopic gastric tumors. Parvoviruses selectively replicate and produce NS1 in tumor cells. After systemic administration of parvoviruses, NS1 protein could not be detected in normal tissues, hence the cytotoxic effects of forced NS1 expression in vital organs were unknown. To assess the efficacy and safety of systemic expression of NS1, we directly injected the pEGFP-C1-NS1 (expressing both EGFP and NS-1 under control of the CMV promoters) into subcutaneously grafted SGC-7901 cells using in vivo jetPEI. The jetPEI is a linear polyethylenimine, which forms complexes with nuclear acids, thereby facilitating their uptake through endocytosis. After implantation of 2×10^7 SGC7901 cells
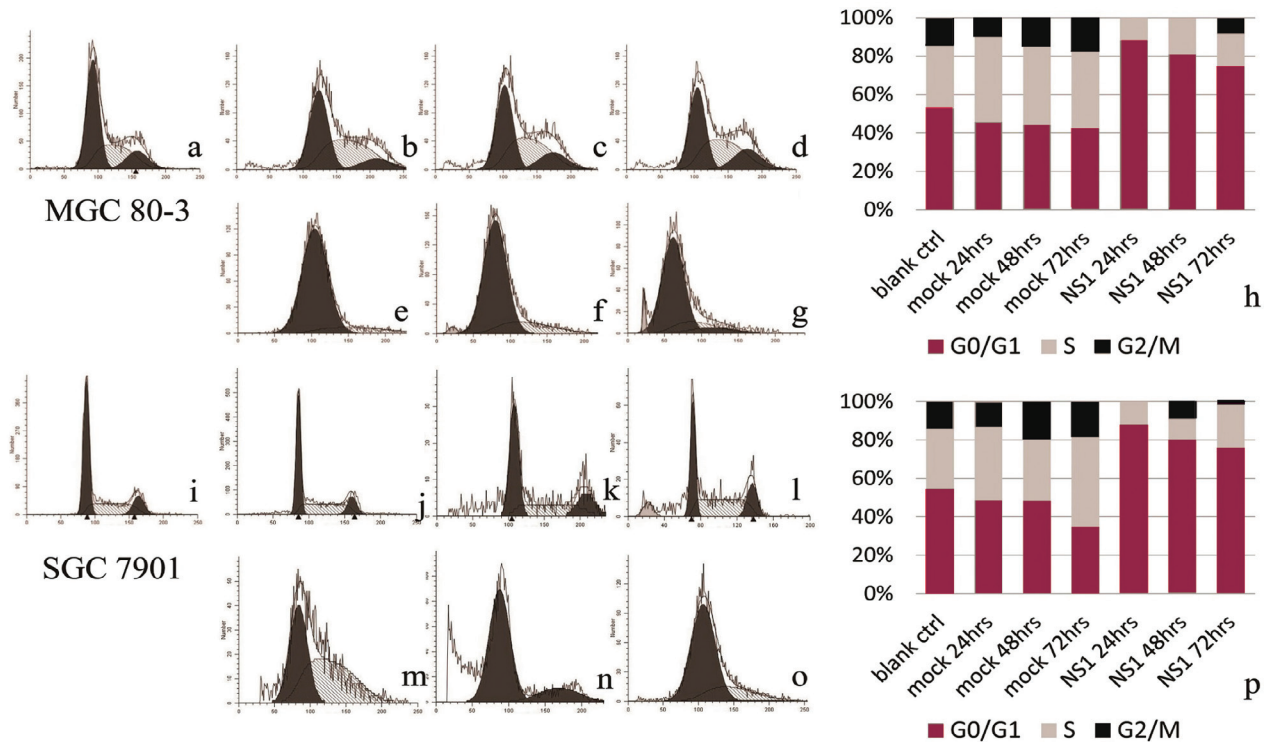
MGC 80-3

SGC 7901

Figure 2 - Nonstructural protein (NS)1-induced cell cycle disturbance as demonstrated by flowcytometry analysis of cell DNA content after propidium iodide staining. All samples were gated on transfected enhanced green fluorescent protein (EGFP)-expressing cells. Upper panel: MGC 80-3 cells; **a)** untreated; **b, c, d)** 24, 48, and 72 hours after treatment with empty carrier pEGFP-C1; **e, f, g)** 24, 48, and 72 hours after treatment with NS1-expressing plasmid (pEGFP-C1-NS1); **h)** cell cycle distribution. Lower panel: SGC 7901 cells; **i)** untreated, j, k, l): 24, 48, and 72 hours after treatment with empty carrier pEGFP-C1; **m, n, o)** 24, 48, and 72 hours after treatment with NS1-expressing plasmid (pEGFP-C1-NS1); **p)** cell cycle distribution presented in stacked percentage column. ctrl - control
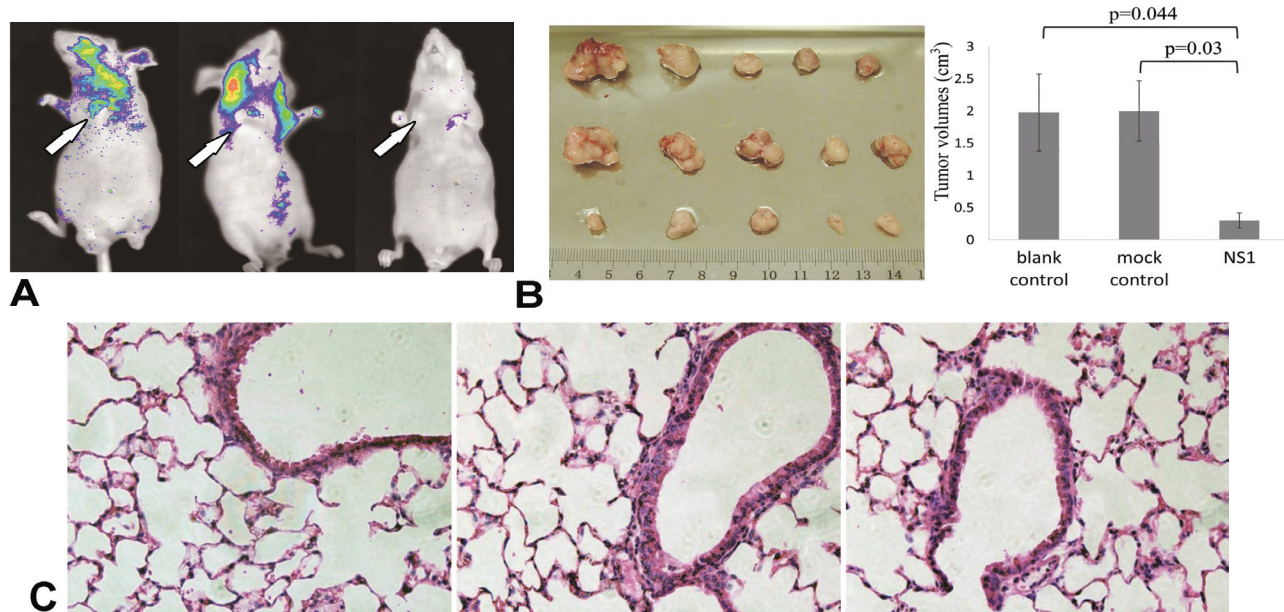

Figure 3 - Heterologous expression of nonstructural protein (NS)1 results in tumor inhibition in vivo. **A)** in vivo tracing of enhanced green fluorescent protein (EGFP) expression in tumor-bearing mice after intra-tumoral injection of expression plasmids. From left to right: mouse injected with empty carrier (pEGFP-C1), mouse injected with recombinant plasmid (pEGFP-C1-NS1), mouse treated with saline, transplanted tumors were marked by arrows; **B)** Tumor excised from NS1 treated and control mice (n=5), left panel (from top to bottom): blank control group, mock control group and NS1 group; right panel: average tumor volumes (with standard deviation bars) in the respective groups; **C)** histological examination of excised lung specimen, from left to right: blank control, mock control, and NS1 group.
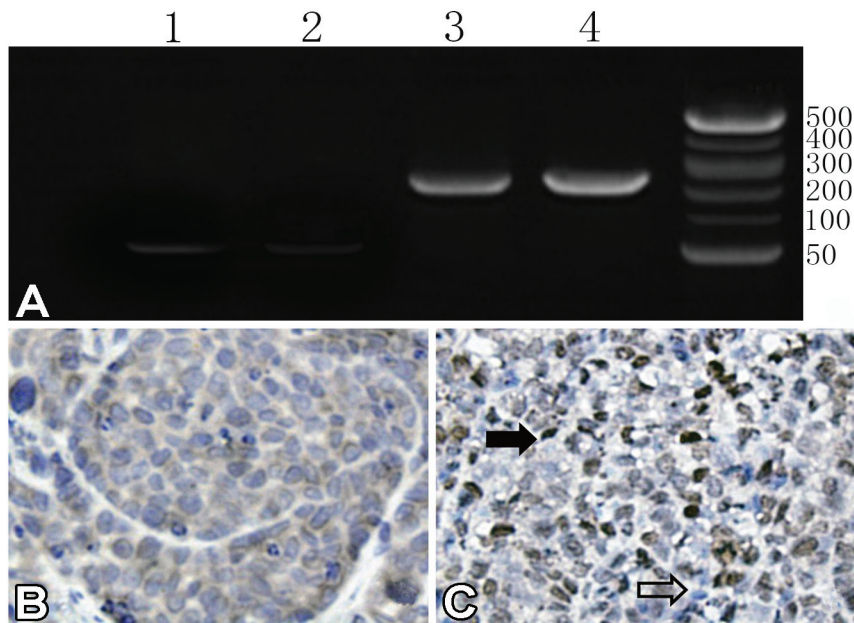
Figure 4 - Detection of in vivo expression of nonstructural protein (NS)1 through analysis of excised tumor samples. **A)** polymerase chain reaction products after 40 cycles of NS1 gene amplification. Lanes 1 and 2: lung (1) and tumor (2) of mock group; lanes 3 and 4: lung (3) and tumor (4) of NS1 group; **B, C)** immunohistochemical detection of NS1 in tumors from mock control and NS1 group(400x). Tumor sample from NS1 group was marked by inflammatory cells infiltration (hollow arrow) and cell debris (black arrow).
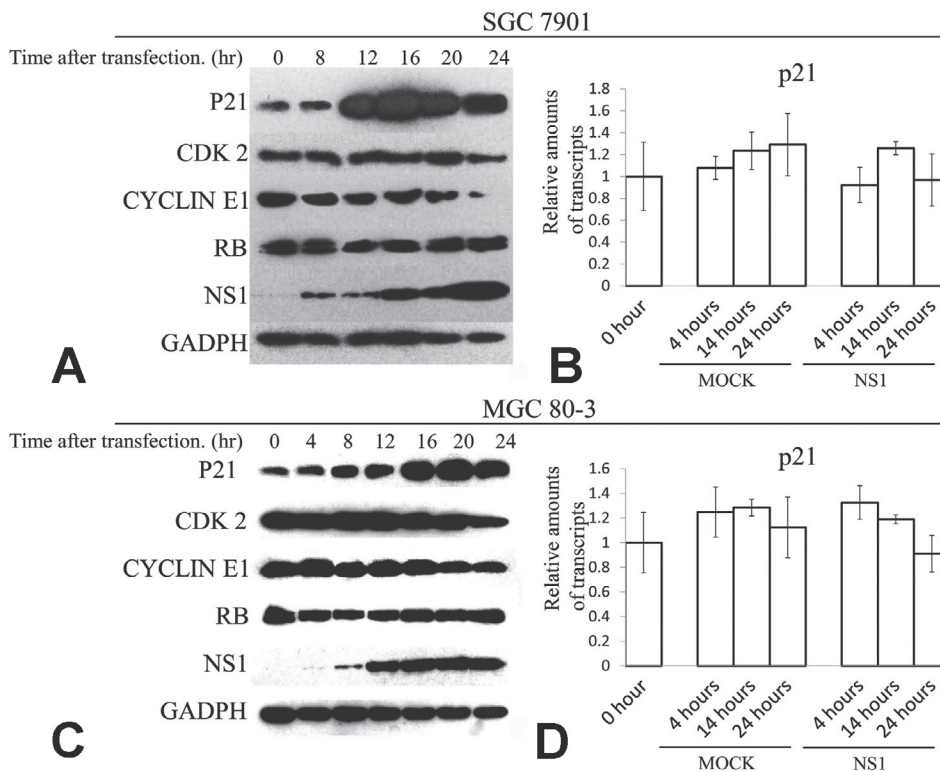

Figure 5 - Effects of nonstructural protein (NS)1 on cell cycle regulators expression in gastric tumor cells. **A, C)** steady state levels of indicated protein in SGC 7901 (**A**) and MGC 80-3 (**C**) cells, as measured by western blotting in function of pEGFP-C1-NS1 transfection time; **B, D)** steady state level of P21 transcripts following pEGFP-C1-NS1 transfection of SGC 7901 (**A**) and MGC 80-3 (**C**) cells, as measured by real time-polymerase chain reaction. Glyceraldehyde-3-phosphate dehydrogenase proteins and messenger RNAs were used as internal controls for data normalization. CDK - cyclin-dependent kinases, RB - retinoblastoma protein, GADPH - glyceraldehyde-3-phosphate dehydrogenase

per mouse, it took approximately 2 weeks for palpable subcutaneous tumors to develop. Plasmid injection was then performed at day 14 post-transplantation, when xenografts reached a section of approximately 0.5x0.5 cm^2. Since in vitro experiments showed that EGFP expression faded away approximately 3 days post transfection, in vivo plasmid injection was repeated 6 times at 72 hours intervals. Mice treated with empty EGFP carrier served as mock, and saline served as blank control. The NS1 expression was traced by in vivo fluorescence imaging. As early as 6 hours after treatment, EGFP expression could be detected in highly vascularized organs such as the lung and brain, besides injected tumor (**Figure 3A**). Both NS1 and mock control groups had similar EGFP expression pattern. During the whole observation period, no apparent adverse effects (death, respiration distress, and abnormal behavior) were observed in either animal groups, giving a first hint that NS1 production (as revealed though EGFP expression and verified below) was harmless when forcefully expressed in healthy lung and brain tissues.

On the second day of the 6-plasmid injection, all the mice were sacrificed for tumor and lung examination. The size of excised tumors was measured using a Vernier caliper. Mice treated with NS1-expressing plasmid exhibited an 85% decrease (p=0.044) of tumor volume compared with empty carrier-treated mice (**Figure 3B**). The latter mock group was un-distinguishable from the blank control regarding tumor sizes. Neither NS1 nor mock-treated animals showed lung abnormalities as judged by the naked eye. After hematoxylin and eosin stain, no structural damage nor inflammatory cells infiltration were found under the microscope (**Figure 3C**).

In vivo plasmid DNA transfection leads to efficient NS1 expression. In a first step, PCR analysis is used to reveal NS1 expression on the RNA level in tissues from plasmid-treated animals. The GAPDH was used as an internal control. After 40 cycles of cDNA amplification, NS1 gene expression was confirmed in both tumor and lung tissues from the experimental group, but was not detected in the mock-treated control group as expected (**Figure 4A**). After being fixed in formaldehyde and cut into 5-10 mm thick sections, tumor samples from both groups were incubated with anti-NS1 antibody to detect in vivo NS1 protein production. Tumors from the NS1 group showed scattered intra-nuclear NS1 expression in tumor cells and surrounding connective tissues. In addition, these tumors could be distinguished by condensed nuclei and cell debris, as well as infiltration of inflammatory cells, which all pointed to tumor necrosis (**Figures 4B** & **4C**).

The NS1-mediated inhibition of gastric tumor cell growth is associated with induction of p21. After in vitro and in vivo validation of NS1's cytotoxic effects on gastric cancer cells, we next investigated the impact of this protein on the expression of key regulators of the cell cycle. It is known that the G1-S transition is controlled by positive (cyclin, cdk) and negative regulators including cdk inhibitor (CKI) and pocket protein family (pRb, for example), and that these proteins are tightly interconnected. This prompted us to compare the NS1-expressing and empty vectors for their effects on the accumulation of some of these regulators as a function of post transfection time. Protein steady state levels of the post-transfection CKI p21 were strongly enhanced from 8-12 hours after transfection of gastric tumor cells with pEGFP-C1-NS1, correlating with the onset of NS1 expression (**Figures 5A** and **5C**). Since SGC7901 and MGC80-3 cells both lack functional p53, a known activator of p21, NS1-mediated induction of p21 appeared to be p53-independent. The protein levels of the other G1-S regulators tested (pRb, cdk2, cyclin E1) were not significantly affected upon NS1 induction. A similar observation was made in both SGC7901 and MGC80-3 cells. Given the known role of p21 in negatively regulating the G1-S transition, the ability of the NS-1 to block this transition may be tentatively traced back, at least in part, to the strong p21 induction achieved by the product. The NS1 is known to be a DNA and protein binding polypeptide, which can trans-activate viral promoters and various host cellular promoters.[21] To determine whether p21 activation in the presence of NS1 was a result of increased gene transcription, total cell RNA was extracted at 4, 14, and 24 hours post transfection, and transcripts were quantitated by RT-PCR. Neither the NS1 nor the mock group showed any significant changes in p21 mRNA levels after transfection, as normalized for GAPDH expression (**Figures 5B** and **5D**). Therefore, the intra-nuclear p21 accumulation taking place in NS1-expressing cells was likely to result from up-regulation at the post-translational level.

Discussion. The ability of parvovirus H-1PV to inhibit the proliferation of human gastric tumor cells has been reported previously.[20] In addition to confirming that this inhibition can be attributed to the parvoviral cytotoxic effector, the NS1 protein, the present study revealed original mechanistic features of this process. The NS1-expressing gastric cancer cells can be blocked in the G1 phase of the cell cycle. This block correlated with the NS1-mediated induction of a known regulator of the G1-S transition, the CKI p21.

The up-regulation of p21 in the presence of NS1 was independent of p53 and took place at a posttranslational level. The interference of a parvovirus (NS1 protein) with cell cycles is not without precedence, and appears to affect different phases, depending on the target cells and experimental conditions, as it was shown recently that NS1 induction in a synchronous HeLa cells predominantly arrested them in G2/M phase of the cell cycle.[16] A similar heterogeneity has also been observed regarding the cell death mechanisms triggered by parvoviruses.[17] The timing of NS1 expression may account for some of these discrepancies, as it depends on the prior entry of cells into the S phase after a genuine parvovirus infection, and on the synchronization of cells undergoing experimental NS1 induction.

In the present study, NS1 was expressed under the control of cell cycle-independent promoters in cells just released from starvation, setting the optimal condition to reveal the interference of NS1 with exit from the G1 phase. It is also worth noting that NS1 is known for its direct, and/or indirect effects on promoter transactivation and mRNA steady state levels.[18]

This work adds another level of complexity to the modes of action of the parvoviral NS1 product, revealing its impact on post-translational regulation of gene expression. The present study shows that in vivo plasmid transfection can be used to efficiently transduce, and express the parvoviral NS1 gene in an animal model. Recombinant plasmid injected into human gastric tumor xenotransplants led to a remarkable suppression of tumor growth in vivo. This result is in agreement with previous reports[5] showing that rodent parvovirus are endowed with oncosuppressive activity, and that the parvoviral NS1 protein is sufficient by itself to cause the lysis of target tumor cells. The NS1-expressing plasmid transfection is at a disadvantage compared with infectious particles infection in that, it is a one-shot procedure, which does not lead to the production of progeny virion, which can spread throughout the tumor via successive rounds of infection. It has to be stated, however, that the inefficiency of intra-tumoral replication and spreading is a common drawback of many oncolytic virions, whose oncosuppressive capacity rather relies on the anti-cancer immune response that takes over from the initial viral oncolytic effect to complete tumor eradication.[19-21] On the other hand, plasmid transfection has a major advantage over virus infection in that, it will not raise the neutralizing antibodies response that is known to be induced by injected viral particles, and to interfere with the repeated administration of these particles.[22,23] The anti-cancer efficiency of in vivo plasmid-mediated transduction of an oncolytic parvoviral protein, as documented, gives further credit to this approach, paving the way for wider application of oncolytic virus through the administration of some of their products.

The oncotropism of parvovirus is multifactorial, and relies in part on the stimulation of the NS1-controlling parvoviral promoter P4 by factors that are activated in malignantly transformed cells.[24,25] Plasmids expressing NS1 under the control of the genuine P4 promoters, may thus be especially suitable for in vivo NS1 transduction, as tumor-specificity of expression and safety are concerned. It should be stated, however, that in the present study, a heterologous promoter was used to program the NS1 gene, resulting in significant NS1 expression in some normal tissues of in vivo transplanted animals, in particular, the lungs and brains. This was not accompanied by any detectable adverse effects, suggesting that other safeguard(s) besides expression regulation protect normal tissues against undesirable cytopathic effects of NS1. These observations are in keeping with previous in vivo data showing that NS1 toxicity is modulated by oncogenic transformation, which can tentatively be traced back to the post-transformed modification of NS1.[24,25]

In conclusion, recombinant plasmid-mediated treatment with the parvoviral protein NS1 appears to meet the efficacy and safety criteria for further validation of this approach. Further work is warranted to develop a more efficient way to introduce NS1 into tumor tissue, as well as elucidate the exact interaction mode of NS1 and the cell cycle regulators.

References

1. Ferlay JSH, Bray F, Forman D, Mathers C, Parkin DM. GLOBOCAN 2008. Cancer incidence and mortality worldwide. IARC CancerBase No. 10. Lyon (France): IARC; 2010. Available from: http://globocan.iarc.fr. 2010
2. China MoHotPsRo. China Health Statistical Yearbook 2012. Mortality Rate of 10 Main Malignant Neoplasms From 2004 to 2005 (1/100 000). Peking (China): Peking Union Medical College Press; 2012.
3. Patel MR, Kratzke RA. Oncolytic virus therapy for cancer: the first wave of translational clinical trials. *Transl Res* 2013 161: 355-364.
4. Rommelaere J, Geletneky K, Angelova AL, Daeffler L, Dinsart C, Kiprianova I, et al. Oncolytic parvoviruses as cancer therapeutics. *Cytokine Growth Factor Rev* 2010; 21: 185-195.
5. Nuesch JP, Lacroix J, Marchini A, Rommelaere J. Molecular pathways: rodent parvoviruses--mechanisms of oncolysis and prospects for clinical cancer treatment. *Clin Cancer Res* 2012; 18: 3516-3523.
6. Lachmann S, Rommeleare J, Nuesch JP. Novel PKCeta is required to activate replicative functions of the major nonstructural protein NS1 of minute virus of mice. *J Virol* 2003; 77: 8048-8060.

7. Bar S, Rommelaere J, Nuesch JP. Vesicular transport of progeny parvovirus particles through ER and Golgi regulates maturation and cytolysis. *PLoS Pathog* 2013; 9: e1003605.

8. Nuesch JP, Rommelaere J. NS1 interaction with CKII alpha: novel protein complex mediating parvovirus-induced cytotoxicity. *J Virol* 2006; 80: 4729-4739.

9. Lacroix J, Schlund F, Leuchs B, Adolph K, Sturm D, Bender S, et al. Oncolytic effects of parvovirus H-1 in medulloblastoma are associated with repression of master regulators of early neurogenesis. *Int J Cancer* 2014; 134: 703-716.

10. Nuesch JP, Lachmann S, Rommelaere J. Selective alterations of the host cell architecture upon infection with parvovirus minute virus of mice. *Virology* 2005; 331: 159-174.

11. Bar S, Daeffler L, Rommelaere J, Nuesch JP. Vesicular egress of non-enveloped lytic parvoviruses depends on gelsolin functioning. *PLoS Pathog* 2008; 4: e1000126.

12. Nuesch JP, Rommelaere J. A viral adaptor protein modulating casein kinase II activity induces cytopathic effects in permissive cells. *Proc Natl Acad Sci U S A* 2007; 104: 12482-12487.

13. Hristov G, Kramer M, Li J, El-Andaloussi N, Mora R, Daeffler L, et al. Through its nonstructural protein NS1, parvovirus H-1 induces apoptosis via accumulation of reactive oxygen species. *J Virol* 2010; 84: 5909-5922.

14. Lachmann S, Bar S, Rommelaere J, Nuesch JP. Parvovirus interference with intracellular signalling: mechanism of PKCeta activation in MVM-infected A9 fibroblasts. *Cell Microbiol* 2008; 10: 755-769.

15. Grekova S, Aprahamian M, Giese N, Schmitt S, Giese T, Falk CS, et al. Immune cells participate in the oncosuppressive activity of parvovirus H-1PV and are activated as a result of their abortive infection with this agent. *Cancer Biol Ther* 2011; 10: 1280-1289.

16. Bhat R, Dempe S, Dinsart C, Rommelaere J. Enhancement of NK cell antitumor responses using an oncolytic parvovirus. *Int J Cancer* 2011; 128: 908-919.

17. Wang YY, Liu J, Zheng Q, Ran ZH, Salome N, Vogel M, et al. Effect of the parvovirus H-1 non-structural protein NS1 on the tumorigenicity of human gastric cancer cells. *J Dig Dis* 2012; 13: 366-373.

18. Nakashima A, Morita E, Saito S, Sugamura K. Human Parvovirus B19 nonstructural protein transactivates the p21/WAF1 through Sp1. *Virology* 2004; 329: 493-504.

19. Shirota T, Kasuya H, Kodera Y, Nishikawa Y, Shikano T, Sahin TT, et al. Oncolytic herpes virus induces effective anti-cancer immunity against murine colon cancer. *Hepatogastroenterology* 2011; 58: 1482-1489.

20. Xiao LL, Wu YM, Qian J, Tan Y, Xie GL, Zhang KJ, et al. The antitumor efficacy of IL-24 mediated by E1A and E1B triple regulated oncolytic adenovirus. *Cancer Biol Ther* 2010; 10: 242-250.

21. Thirukkumaran C, Morris DG. Oncolytic viral therapy using reovirus. *Methods Mol Biol* 2009; 542: 607-634.

22. Muharemagic D, Labib M, Ghobadloo SM, Zamay AS, Bell JC, Berezovski MV. Anti-Fab aptamers for shielding virus from neutralizing antibodies. *J Am Chem Soc* 2012; 134: 17168-17177.

23. Pesonen S, Diaconu I, Kangasniemi L, Ranki T, Kanerva A, Pesonen SK, et al. Oncolytic immunotherapy of advanced solid tumors with a CD40L-expressing replicating adenovirus: assessment of safety and immunologic responses in patients. *Cancer Res* 2012; 72: 1621-1631.

24. Ventoso I, Berlanga JJ, Almendral JM. Translation control by protein kinase R restricts minute virus of mice infection: role in parvovirus oncolysis. *J Virol* 2010; 84: 5043-5051.

25. Grekova S, Zawatzky R, Horlein R, Ciepluch C, Mincberg M, Davis C, et al. Activation of an antiviral response in normal but not transformed mouse cells: a new determinant of minute virus of mice oncotropism. *J Virol* 2010; 84: 516-531.

Related Articles

Pu YW, Gong W, Wu YY, Chen Q, He TF, Xing CG. Proximal gastrectomy versus total gastrectomy for proximal gastric carcinoma. *A meta-analysis on postoperative complications, 5-year survival, and recurrence rate. Saudi Med J* 2013; 34: 1223-1228.

Ge Z, Zhao C, Wang Y, Qian J. Cholecystectomy and the risk of esophageal and gastric cancer. *Saudi Med J* 2012; 33: 1073-1079.

Al-Khattaf AS. Helicobacter pylori virulence markers in gastroduodenal disorders. *Detection of cytotoxin-associated gene A and vacuolating cytotoxin-associated gene A genes in Saudi patients. Saudi Med J* 2012; 33: 716-721.